

## CHAPTER I

### INTRODUCTION



The experimental and theoretical investigations on heavily doped semiconductors have marked a considerable progress in the recent years. This is due to the fact that such materials are technologically important and, at the same time they pose challenging problems with implication reaching far beyond the field itself. The technological applications of such heavily doped semiconductors go well outside the tunnel diode.<sup>1</sup> These semiconductors are also used in laser<sup>2</sup>, in thermoelectric devices, in semiconductor catalysts, and some active components of solid-state systems<sup>1</sup>. A second reason for the interest is the significant progress towards an understanding the disordered materials. One extreme case of heavily doped semiconductors is that of disorder alloys<sup>3</sup>.

A serious study of heavily doped semiconductors started about 20 years ago<sup>4</sup>, it was stimulated by the invention of a number of devices in which an important role is played by electronic states that are produced in the forbidden band under the influence of impurities. The new property of these impure crystals is discovered when the techniques for preparing pure semiconductor single crystal are developed. While the gradual reduction of impurity concentration is achieved it has become clear that the technology of semiconductor

devices requires not simply crystals of maximum purity but crystals with impurities introduced deliberately in precisely known amounts, which are called "doped semiconductors."<sup>5</sup>

In this thesis, the density of states available to electrons in heavily doped semiconductors is studied because many quantities such as, Fermi energy<sup>6</sup>, energy gap<sup>7</sup> can be determined from this density of states. Electron in a perfect, imperfect crystal, and heavily doped semiconductors will be considered respectively.

### 1.1 Perfect crystals

The common characteristic of the perfect crystals is their periodicity, which implies perfect ordering of the atoms in regard to their position, composition and orientation (for non spherically symmetric atoms) both on an atomic, or short, scale and on a macroscopic, or long, scale. The potential seen by the single conduction electron is the same at every point in the crystal and is taken as periodic with the period of the crystal lattice. The potential function for a one dimensional model is shown in Fig. 1.1a as a linear array of positive ionic "cores".

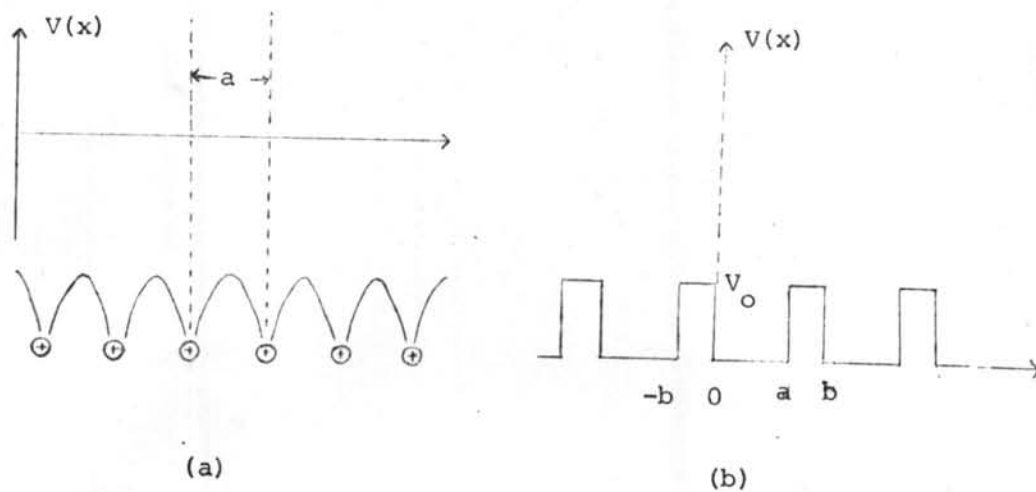


Fig. 1.1 The one-dimensional perfect crystal potential  $V(x)$  as a function of position  $x$ .

(a) The true potential

(b) The Kronig and Penney square potential

Of course, the precise nature of  $V(x)$  is complex and the solution of Schrödinger equation including such a function is complicated. However, Kronig and Penney<sup>8</sup> made certain simplification which makes the mathematics manageable,  $V(x)$  is approximated by the series of square potential wells as shown in Fig 1.1b. In regions for which  $x$  lies between zero and  $a$ , the potential energy of the electron is assumed to be zero, and in regions for which  $x$  lies between  $-b$  and zero the potential energy is taken as  $V_0$ . The value of the Kronig and Penney model is that it enables one to take two Schrödinger equations for the different regions.

$$\frac{d^2\psi}{dx^2} + \left(\frac{2mE}{\hbar^2}\right)\psi = 0 \quad \text{for } 0 \leq x \leq a \quad (1.1.1)$$

and

$$\frac{d^2\psi}{dx^2} + \left(\frac{2m}{\hbar^2}\right)(E - V_0)\psi = 0 \quad \text{for } -b \leq x \leq 0 \quad (1.1.2)$$

For simplicity, let the width of barriers,  $b$ , go to zero and their height to infinity, in such a way that the strength of the barrier remains constant, or in other words, the potential is considered to be a periodic delta function. Bloch showed that the solutions of (1.1.1) and (1.1.2) are then of the form<sup>9</sup>

$$\psi(x) = U(x)e^{i\alpha x}, \quad \alpha = 2\pi K/L \quad (1.1.3)$$

where  $K$  is any integer and  $U(x)$ , called a Bloch function, is a function periodic in  $x$  with the period  $(a+b)$  and  $L = G(a+b)$  where  $G$  is a large integer. When the usual boundary conditions of  $\psi(x)$  and  $\partial\psi(x)/\partial x$  are applied, it is found that (1.1.3) is only a solution for particular value of electron energy  $E$  which satisfies the equation

$$P \sin(\beta a)/\beta a + \cos(\beta a) = \cos(\alpha a) \quad (1.1.4)$$

where  $\lim_{\substack{b \rightarrow 0 \\ \gamma \rightarrow 0}} \frac{\gamma^2 ab}{2} = P$ ,  $\gamma = [(2m/\hbar^2)(V_0 - E)]^{1/2}$  and  $\beta = [(2m/\hbar^2)E]^{1/2}$

It is noted that the energy spectrum of the electron consists of continuous bands at allowed level separated by forbidden gaps,  $E_g$  as depicted in Fig. 1.2a.

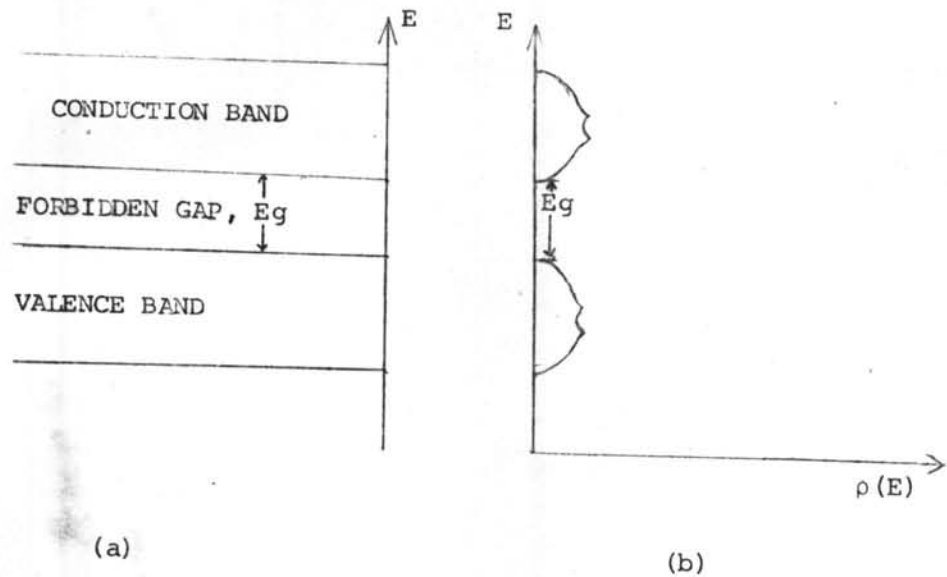


Fig. 1.2 Energy band scheme of perfect crystal.

- (a) Simplified band structure of perfect crystal  
 (b) Density of states  $\rho(E)$  as a function of energy  $E$  for a perfect crystal.

When the electrons are added to the solid, the electrons fill up the lowest energy bands first. The highest energy band that is completely filled is called the "valence" band and the unfilled or partly filled band is called the "conduction" band. In this



band the electrons can readily change momentum states in an applied electric field and contribute to a net flow of electrons (electrical conductivity) in a crystal.

The electronic energy bands provide the basis for electrical classification of solid as metal, semiconductor and insulator. An insulator is a solid which the valence band is full, the conduction band is empty and the energy gap,  $E_g$ , between them is too large to excite electrons across  $E_g$ . In metal, either the valence and the conduction bands overlap, so that both are partially filled, or else the highest band is only half-filled because the atoms, e.g. Na, have an odd number of electrons. In semiconductor, there are only a few electrons in the conduction band or a few unfilled states (holes) in valence band which makes only limited conduction possible. In the last case the size of  $E_g$  is the most important.

The density of states  $\rho(E)$  for the perfect crystal, in the so-called parabolic band approximation, is the same as the result for no spatial variation of potential energy (Sommerfeld model)<sup>10</sup>. However, the free electron mass  $m_0$  is replaced by the effective mass  $m^*$  which gives<sup>9</sup>

$$\rho(E) = 4\pi \left(\frac{2m^*}{h^2}\right)^{3/2} E^{1/2} \quad (1.1.5)$$

with  $E$  the energy in electron volts. Equation (1.1.5) is shown

in Fig. 1.2 (b) for equal electron and hole effective mass and an arbitrary band gap  $E_g$ .

## 1.2 Imperfect Crystals

When impurities are introduced into the periodic crystal, for example into pure semiconductor, the perfect periodicity of the potential will be destroyed. Each impurity atom gives rise to a new isolated impurity level in the forbidden energy gap. The deliberate addition of controlled quantities of these impurity elements is called "doping"<sup>5</sup>. The doped semiconductors are classified into main categories, according to the type of charge carrier which predominates, n-type and p-type semiconductors<sup>11</sup>.

When an impurity, such as an atom of phosphorus having five valence electrons, is substituted for a silicon atom in a pure silicon crystal, the single electron in excess of the four valence electrons required for the covalent bonding of the silicon lattice, becomes free and moves away from the host phosphorus atom. The phosphorus atom that is thus missing one electron necessary to make it neutral and is fixed in position as a positive ion in the crystal is called a "donor". Since the current carrier is the negative excess electron, the silicon is said to be an n-type semiconductor, and the phosphorus is called an n-type impurity, which forms donor level below the conduction band. A similar situation can be produced in the opposite

direction by introducing an atom of a Group III metal, such as boron in silicon. The boron has three valence electrons and is therefore deficient by one electron required to reconstruct the covalent bond in the silicon lattice. To make up this deficiency, the boron atom accepts one electron from the rest of the crystal, leaving a hole that becomes free and moves away from the boron atom. The boron atom that has thus gained one electron and is fixed in position as a negative ion in the crystal is called an "acceptor". Since the current carrier is the positive excess hole, the silicon is said to be a p-type semiconductor, and the boron atom is called a p-type impurity which forms an acceptor level in the forbidden gap above the valence band.

For a low density of impurity atoms, the impurity ions are separated far enough from each other such that there is no interaction among the various impurities. In such a situation, each ion can be considered as a separate physical system. For these isolated donor and acceptor systems under thermal-equilibrium condition, the donor and acceptor levels are calculated by using the hydrogenic model. For an isotropic material with dielectric constant  $\epsilon$ , the effect of host atoms can be crudely explained in terms of effective mass  $m_e^*$  (for an electron) and  $m_h^*$  (for a hole). By solving the Schrödinger equation with hydrogenic Hamiltonian one obtains the donor and acceptor states lying at energies,

$$E_d = m_e^* e^4 / 2h^2 \epsilon^2 \quad (1.2.1)$$



and

$$E_a = \frac{m_h^* e^4}{2h^2 \epsilon^2} \quad (1.2.2)$$

below the conduction and above the valence band edges respectively.

Hence, it is to be noted that, there will be a non-zero density of states inside the gap with a peak expected around the position of the bound state corresponding to a single impurity as depicted in Fig 1.3a

### 1.3 Heavily Doped Semiconductors

In the low-doping system<sup>13</sup>, as mention in sec 1.2, the isolated impurity ion has been described using the hydrogenic model resulting in the introduction of a discrete energy level in the forbidden energy gap. As the number of impurity ions increase, eventually the hydrogen-like wavefunctions on adjacent ions overlap and interact causing the broadening of the discrete level ( Fig 1.3b ). For a doping concentration at which the discrete level is beginning to broaden the center of the impurity band is expected to be the same as the position of the discrete level. As one increases the doping, the screening length is increased due to the carriers from the ionized dopants. The whole band then shifts towards the adjacent main band in the same way that the discrete level moves toward the adjacent band. When the center of the impurity band merges into the main band, the two

entities become one with a parabolic main band plus a tail. This defined the "heavily doped", or, in other word, a semiconductor is considered heavily doped when the impurity band associated with the doped impurity merges with either the conduction or the valence band<sup>14,15</sup> see Fig 1.3c.

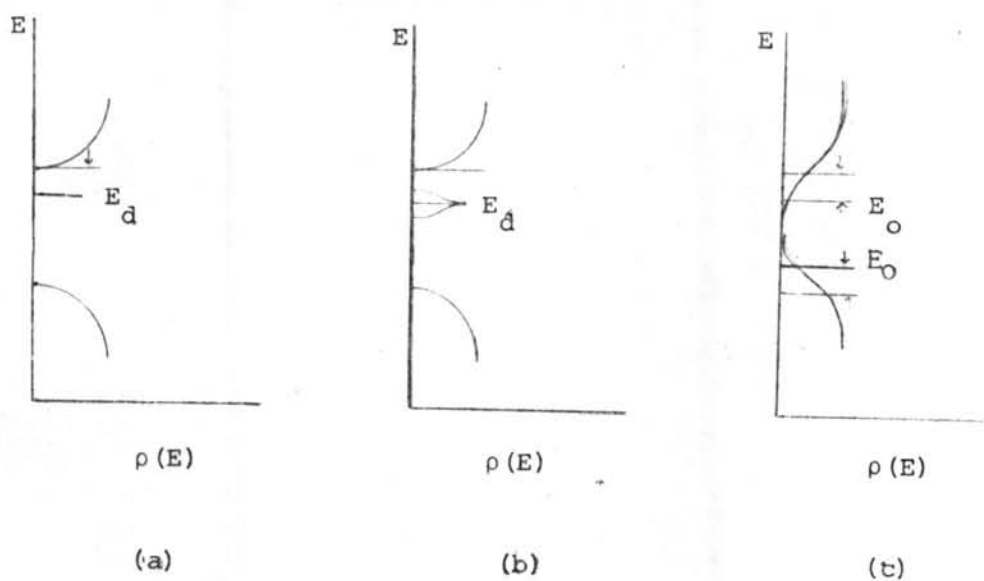


Fig. 1.3 The density of states  $\rho(E)$  as a function of energy  $E$

- (a) Single impurity atom.
- (b) Low impurity concentration localized impurity level located at an energy level  $E_d$  below the conduction band.
- (c) Heavily doped semiconductor-merged impurity band showing the band tails and the shift of the band edges  $E_0$ .

Evidence for band tails in the forbidden band of heavily doped semiconductors was provided by the number of experiments on tunneling<sup>16</sup>, optical absorption<sup>17</sup> and luminescence<sup>18</sup>. The electronic properties of heavily doped semiconductor depends largely on the tail in density of states. For this reason theories of impured semiconductors focussed on determining density of states in this tail. For one-dimensional, Lax and Phillips<sup>19</sup>, and Frish and Lloyd<sup>20</sup> consider the impurity potentials as the  $\delta$ -functions. Quantitative three-dimensional calculations have been performed by Parmenter<sup>21</sup> using Perturbation theory and assuming a screened Coulomb model for impurities. More recently Wolff<sup>22</sup> has used a more rigorous perturbation type approach. He treats electron-electron effects ab-initio and justifies the screened Coulomb model for the impurities in the high concentration limit. However, the perturbation techniques lead to the tail that cut off sharply.

Kane<sup>23</sup> has combined the potential energy fluctuations with the Thomas-Fermi method<sup>10, 24</sup> or semi-classical method, to calculate the density of states. In this method he assumes that the local potential is sufficiently slowly varying that the local density of states can be defined just as if the potential were constant. The calculation of the over all density of states then reduces to the calculation of the distribution function. It is noticed that the potential energy fluctuations at high concentrations are Gaussian, the tail found by Kane is Gaussian. Owing to the omission of the

kinetic energy of localization in the Thomas-Fermi method, the density of states obtained from Kane Theory lead to the overestimated value.

$$\rho(E) = y(E/\eta) m^{*3/2} (2\eta)^{1/2} V \pi^{-2} \hbar^{-3} \quad (1.3.1)$$

$$\text{where } y(x) = \pi^{-1/2} \int_{-\infty}^x (x-\xi)^{1/2} \exp(-\xi^2) d\xi$$

The most complete calculation of density of states in the low energy, deep tail region of the impurity-band remains the optimal fluctuation results of Halperin and Lax theory<sup>25,26</sup>. Their theory is the quantum counterpart of the original semi-classical theory of Kane. Quantum effects were included by adding the zero point energy of the electron states (kinetic energy of localization) which raises the electron state energies and reduced density of states at small energy below the semiclassical value obtained by Kane.

More recently, Sa-yakanit<sup>27-29</sup> has used the Feynman path integral technique<sup>30</sup> to achieve an analytical form of density of states. The density of states evaluated by this method agree with that evaluated by Halperin and Lax<sup>25</sup> i.e.,

$$\rho(E) = [A(E)/\xi^2] \exp[-B(E)/2\xi] \quad (1.3.2)$$

The functions  $A(E)$  and  $B(E)$  evaluated by path integral method are expressed analytically in terms of parabolic cylinder function. Although, it is difficult to obtain the numerical values of this function, but it is more convenient to calculate the density of states by evaluating the parabolic-cylinder function than by numerical solving Hartree-Fock equation as was done by Halperin and Lax<sup>25</sup>.

The most simply method, which provides one with analytical and easily usable expressions for the density of states tails, and which enables one to derive the validity condition of the last two theories very clearly, is obtained by guessing an appropriate trial wavefunction of Schrödinger equation. By this method Eymard and Duraffourg<sup>31</sup> used the simple Hydrogen-like wave function and applied the variational principle to adjust the parameter of the wave function in order to maximize the density of states. They received an analytical density of states with the simple form. Because their trial wave function is the simple one hence their results are only in a good agreement with the computed Halperin and Lax results in the range of small values of  $\xi' = \xi/E^2$ <sub>Q</sub>.

In this thesis, the density of states is evaluated analytically by using the two different potentials, the screened Coulomb potential and the Gaussian potential. For the case of the screened Coulomb potential, the new appropriate wave function is chosen which does not only give the better results but is also as easily usable a calculation as Eymard and Duraffourg method<sup>31</sup>. For the case of Gaussian potential, the ground state Gaussian wave function is used. The detail of these

methods is shown in chapter III. Halperin and Lax Theory<sup>25</sup> and Sa-yakanit Theory<sup>27-29,32</sup> are presented in Chapter II. Discussions and a detailed comparison of present methods with Eymard and Duraffourg method<sup>31</sup>, Halperin and Lax Theory<sup>25</sup>, and Sa-yakanit Theory<sup>29</sup> are presented in chapter IV. The computer programs using to obtain the numerical results for Eymard and Duraffourg method and present methods are given in Appendix A, B and C respectively.